JOURNAL OF MATERIALS SCIENCE **34** (1999) 2859–2864

Carbide behaviour during high temperature low cycle fatigue in a cobalt-base superalloy

W.H. JIANG*
Institute of Metal Research, The Chinese Academy of Sciences, 72 Wenhua Road, Shenyang 110015, People's Republic of China; Department of Metal Materials Engineering, Shenyang Polytechnic University, 50 Xinghua Street, Shenyang 110023, People's Republic of China

X.D. YAO, H.R. GUAN, Z. Q. HU
Institute of Metal Research, The Chinese Academy of Sciences, 72 Wenhua Road, Shenyang 110015, People's Republic of China
E-mail: zqhu@imr.ac.cn

The carbide behaviour of a directionally solidified cobalt-base superalloy has been investigated after low cycle fatigue at 900 °C. During fatigue, primary carbides, M_7C_3 and MC, decomposed sluggishly and a great amount of secondary carbide, chromium-rich $M_{23}C_6$ precipitated. The inhomogeneous distribution of $M_{23}C_6$ brought about a different dislocation substructure. In the vicinity of the primary carbides, densely-distributed fine $M_{23}C_6$ pinned up dislocations effectively, resulting in a uniform distribution of dislocations, while in the interior of grains, since precipitates were coarse and scarce, dislocations were arranged in a planar array and piled up in the front of the precipitates. $M_{23}C_6$ also acted as an obstacle deflecting fatigue crack. Primary carbides on the surface of specimens were oxidizied preferentially, causing a precipitate depletion around them. The oxidized primary carbides were crack initiation sites. The primary carbides hindered fatigue crack propagation, causing the formation of shear steps.

1. Introduction

Cast cobalt-base superalloys are widely used in many military and commercial aircraft turbine engines for vanes and other high temperature structural components. The choice for use of those materials in gas turbine application is primarily based on a good combination of their high rupture stress and excellent hot corrosion resistance after prolonged exposure.

The presence of carbide phase has long been recognized as an important strengthening mechanism in cast cobalt-base superalloys. Historically, carbide strengthening has been associated with coarse primary carbides and fine secondary carbides. In as-cast condition, they only contain primary carbides located at grain boundaries and interdendritic regions. Subsequent exposure to high temperature may induce secondary carbide precipitation. The primary carbides inhibit grain boundary sliding at elevated temperature, while fine secondary carbides exert a direct interaction with dislocations. They contribute significantly to strengthening [1]. In fact, heat treatment is hardly applied to cast cobalt-base superalloys and they are frequently put into use in a thermodynamically unstable condition. Therefore, it is essential to understand their microstructural change during service at high temperature.

In gas turbine application, the components are subjected to repeated thermal stresses as a result of temperature changes which occur during startups, thrust changes, and shutdowns. Therefore, high temperature fatigue behaviour of superalloys has been the object of numerous studies. Particularly, much attention has been paid to cyclic strain-induced microstructural changes. For example, Antolovich and Jayaraman [2] observed carbide precipitation during high temperature low cycle fatigue in a nickel-base superalloy, Waspaloy. Unlike nickel-base superalloys, cast cobalt-base superalloys are principally strengthened by dispersion of carbide precipitates. So, it can be expected that carbide precipitates have a beneficial effect on improving high temperature low cycle fatigue resistance. However, so far, little information is available in this respect. The present work investigated carbide evolution of a directionally solidified cobalt-base superalloy during low cycle fatigue at 900 °C and effect of carbide phases on deformation and fracture.

2. Experimental

The alloy studied was prepared in a conventional vacuum unidirectional solidification furnace with mould

* Author to whom all correspondence should be addressed: 6th Department, Institute of Metal Research, the Chinese Academy of Sciences, 72 Wenhua Road, Shenyang 110015, People's Republic of China.

TABLE I Nominal composition of the alloy

	Cr	Ni	W	Mo	Ta	Ti	Zr	Al	B	C	Co
wt %	25	11	7.5	0.2	0.25	0.15	0.15	0.8	0.05	0.45	bal

withdrawal device. The nominal composition of the alloy is listed in Table I. Cylindrical rods of the alloy, 16 mm in diameter and 140 mm long, were produced at a withdrawal rate of 7 mm/min and with a thermal gradient of 50–60 K/cm at the solid/liquid interface.

Specimens with a gage length of 10 mm and a diameter of 6 mm were machined from the as-cast bars. The low cycle fatigue tests were performed under fully reversed, axial stress control mode, at a frequency of 0.15 Hz, in a servohydraulic system. The tests were conducted in air at 900 °C.

The fracture surface of fatigued samples was examined by scanning electron microscopy (SEM) to determine the crack initiation and the propagation mode. Studies were also conducted on longitudinal sections of broken specimens to document the microstructural changes that occurred during testing. Energy dispersive analysis of X-rays was used to determine local chemical composition. Secondary carbides and deformation-induced substructures were studied by transmission electron microscopy (TEM). Samples for TEM examination were obtained from thin slices cut at a distance of 1 mm away from the fracture surface. The slices were mechanically thinned down to 50 μm and then electropolished in a solution containing 5% perchloric acid and 95% methanol at about −20 °C in a twin-jet apparatus. Thin foils were examined in an electron microscope operating at an acceleration voltage of 100 keV. The orientation of TEM foils was normal to the loading axis.

3. Results and discussion

3.1. Carbide characteristic

Fig. 1 shows the microstructure of the as-cast alloy. The alloy matrix is a well-developed columnar grained austenite with ⟨0 0 1⟩ direction parallel to the growth axis. X-ray diffraction analysis and energy dispersive X-ray analysis indicated that the alloy contained two types of primary carbides, i.e. chromium-rich M_7C_3 and MC composed of Ta, Ti, Zr and W [3]. The scanning electron image (Fig. 2) shows their morphologies and distributions. In this backscattered electron image, the chromium-rich M_7C_3 carbide appears dark and the MC carbide is rather light. It can be seen that the M_7C_3 carbide is in the form of rods or irregular aggregates, while MC is present as a discrete, blocky dispersion and a well distributed Chinese script morphology. Both M_7C_3 and MC carbides are situated at grain boundaries and interdendritic regions, forming a continuous network around the columnar grained matrix.

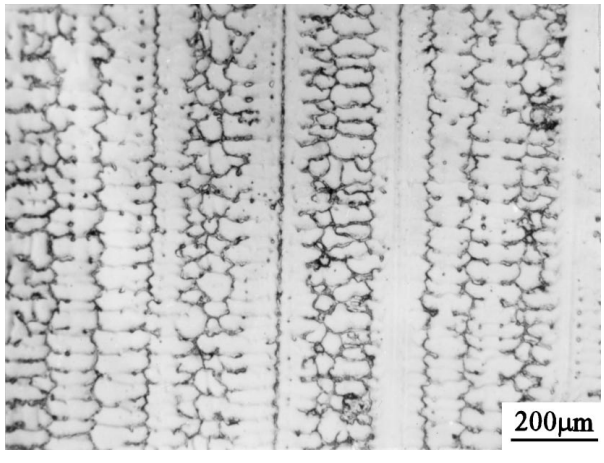

Figure 1 Optical micrograph of the as-cast alloy showing a columnar grained structure in longitudinal cross section.

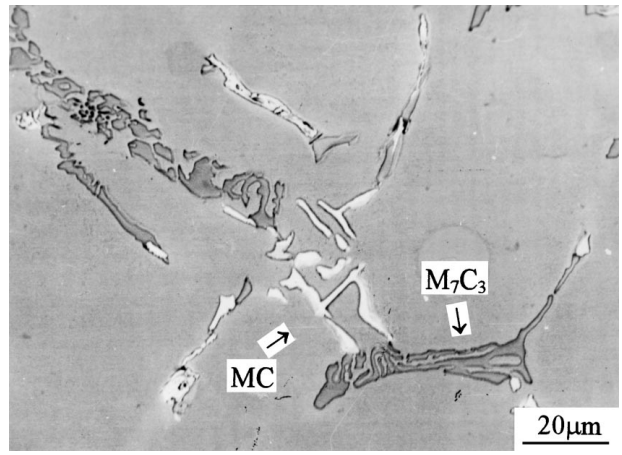

Figure 2 Backscattered electron micrograph of primary carbides in the as-cast alloy in transverse cross section.

The present alloy is similar to classical X-40 in chemical composition except the minor addition of reactive elements. Although there is only one kind of primary carbide, $M_{23}C_6$, in the conventional equiaxed as-cast X-40 alloy [4], the primary carbide of M_7C_3 was also found in a directionally solidified X-40 [5]. This demonstrates that directional solidification not only modifies grain structure of alloy matrix and carbide distribution, but also has an effect on the nature of primary carbides. MC carbide is usually found in contemporary high strength cobalt-base superalloy, such as MAR-M509 alloy, which has a relatively high content of reactive elements, up to 4 wt % [4]. However, the minor addition of reactive elements, Ta, Ti, Zr, summing only 0.55 wt %, also caused the formation of the MC type carbide in the alloy. Consequently, the carbide characteristic of the as-cast DZ40M alloy has an intimate relationship with the application of the directional solidification technique and the modification in the alloy composition.

A substantial microstructural change has occurred in broken specimens even with the shortest fatigue life, $N_f = 205$ cycles. Fig. 3 is a typical microstructure of the broken specimen. From Fig. 3a, it can be seen that the primary carbides have thinned out, indicating their dissolution and a profusion of secondary precipitates were produced. Fig. 3b exhibits that the secondary precipitates are unevenly distributed. Close to the primary carbides, both M_7C_3 and MC, there is a dense distribution of very fine precipitates. In the interior of austenite

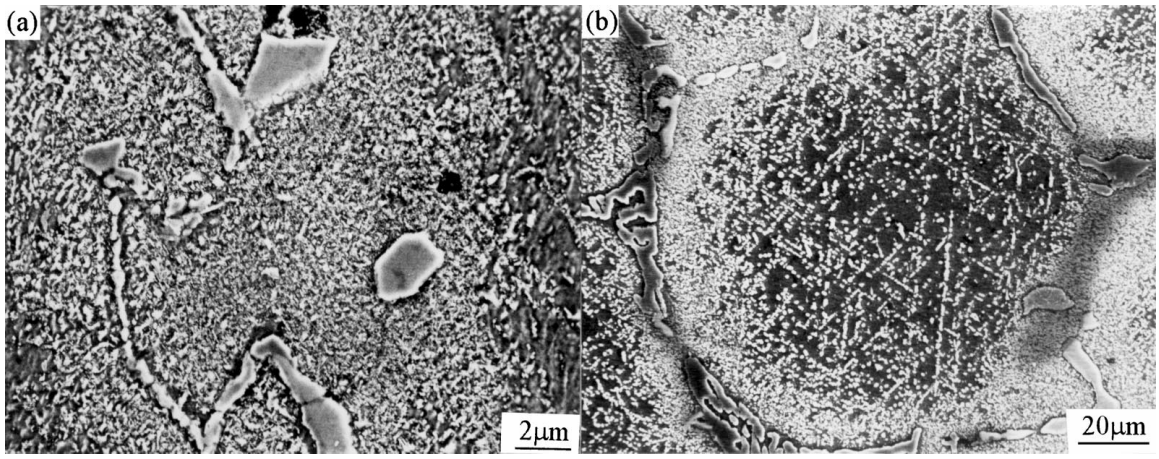

Figure 3 Scanning electron micrographs showing (a) dissolution of primary carbides and secondary precipitates and (b) distribution of secondary precipitates in a broken specimen, at $\sigma = 200$ MPa, $N_f = 1.92 \times 10^4$ cycles.

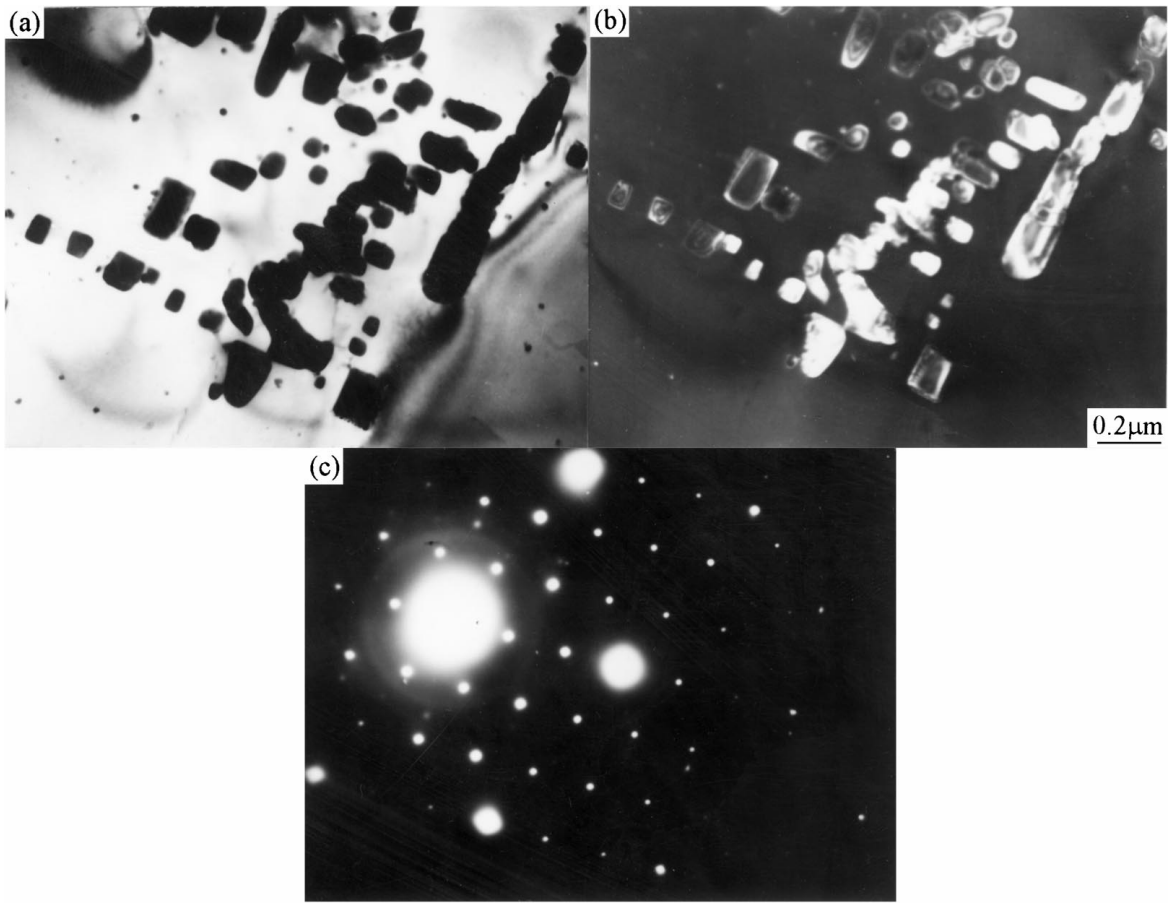

Figure 4 (a) Bright field transmission electron micrograph of the fine precipitates formed after test at $\sigma = 200$ MPa, $N_f = 1.92 \times 10^4$ cycles, (b) Dark field micrograph of the same region, using {311} precipitate reflection and (c) Corresponding diffraction pattern showing a cube-cube matrix: precipitate relationship.

grains, coarser secondary precipitates are aligned in rows. Energy dispersive analysis of X-rays indicated that they were rich in chromium.

Transmission electron micrographs (Fig. 4a and b) display that the precipitates have a cuboidal morphology and some have coalesced into platelets. The electron diffraction analysis (Fig. 4c) demonstrates that all these precipitates possess the same crystal structure and their characteristic reflections are present at every one-third position of the fcc matrix reflections. This indicates that the precipitates have a fcc structure with a lattice constant that is nearly three times that of the matrix, and they also assume a cube-cube orientation relationship with the matrix:

$$\{100\}_{\text{precipitate}} // \{100\}_{\text{matrix}}$$
$$\langle 100\rangle_{\text{precipitate}} // \langle 100\rangle_{\text{matrix}}$$

These are characteristic feature of the chromium-rich $M_{23}C_6$ carbide [6].

During low cycle fatigue at 900 °C, the dissolution of the primary carbides, M_7C_3 and MC, and the profusive precipitation of secondary carbide have happened.

A carbide transformation is a common phenomenon in cobalt-base superalloys, for they rarely reach a thermodynamical equilibrium condition before long term service, or in the absence of heat treatment [4]. Compared with the primary ones, M_7C_3 and MC, the secondary $M_{23}C_6$ carbide appears to be more thermodynamically stable. The heavy precipitation of the secondary $M_{23}C_6$ carbide surrounding the primary carbides indicates that it is closely related to the decomposition of the primary ones. Lane and Grant [7] proposed that Cr_7C_3 was metastable and decomposed into $Cr_{23}C_6$ through an *in situ* reaction, i.e.

$$23Cr_7C_3 \rightarrow 7Cr_{23}C_6 + 27C \quad (1)$$

Subsequently, the carbon atoms released by this reaction diffused locally into alloy matrix, combining with more chromium to form fine precipates as follows:

$$6C + 23Cr \rightarrow Cr_{23}C_6 \quad (1a)$$

Concerning the degeneration of the primary MC into the secondary $M_{23}C_6$, Sims [4] suggested a relatively direct reaction, that is,

$$MC + \gamma \rightarrow M_{23}C_6 \quad (2)$$

Lately, the present authors [3] investigated the carbide change in as-cast DZ40M alloy after long term thermal exposure at 850 °C, and proposed a direct element reaction for the precipitation of $M_{23}C_6$, i.e.

$$23M + 6C \rightarrow M_{23}C_6 \quad (3)$$

As a carbon reservoir, the primary carbides provided carbon atoms for the precipitation reaction. It is reasonable to deduce that during low cycle fatigue at 900 °C, the precipitation of $M_{23}C_6$ in DZ40M alloy followed the same mechanism as reaction (3). Undoubtedly, cyclic stress favored the carbide transformation.

In the interior of grains, the precipitation of $M_{23}C_6$ carbide preferentially occurred on dislocations and stacking faults, as shown in Fig. 5. This confirms that it was induced by cyclic stress during fatigue. It is well known that dislocations and stacking faults can significantly reduce the activation energy for precipitation and solute atoms have a tendancy to segregate there, forming a local segregation zone. In so doing, they act as favorable sites of $M_{23}C_6$ precipitation. Cyclic stress not only can produce dislocations and stacking faults, but also can accelerate the diffusion of solute atoms, that promotes the precipitation of $M_{23}C_6$ during fatigue. Subsequently, $M_{23}C_6$ in the interior of grains grew and coalesced into platelets (Fig. 3b).

Fig. 6 shows that the surface of the specimen is severely oxidized after fatigue. In particular, it should be noticed that the preferential oxidation of the primary carbides has occurred. Furthermore, it could be observed that there is a precipitate-depleted zone below the oxidization layer. During low cycle fatigue at 900 °C in air, the surface of specimens suffered a severe oxidation and particularly, the primary carbides were preferentially oxidized. Oxidation devoured the primary carbides on the surface of specimens and the loss of carbon reservoir inhibited the precipitation of $M_{23}C_6$, resulting in the formation of a precipitate-depleted zone around them.

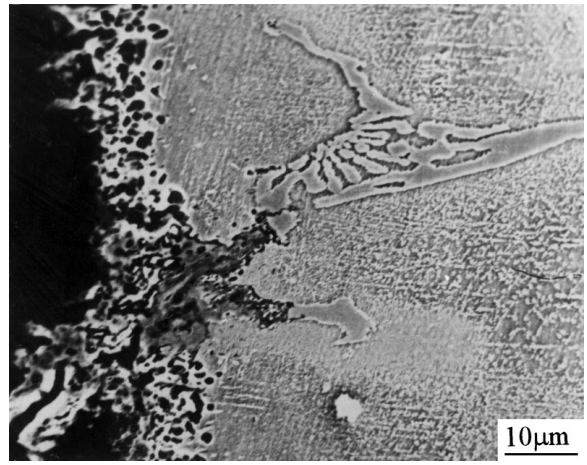

Figure 6 SEM micrograph showing the oxidation of a specimen surface after test at $\sigma = 200$ MPa, $N_f = 1.92 \times 10^4$ cycles.

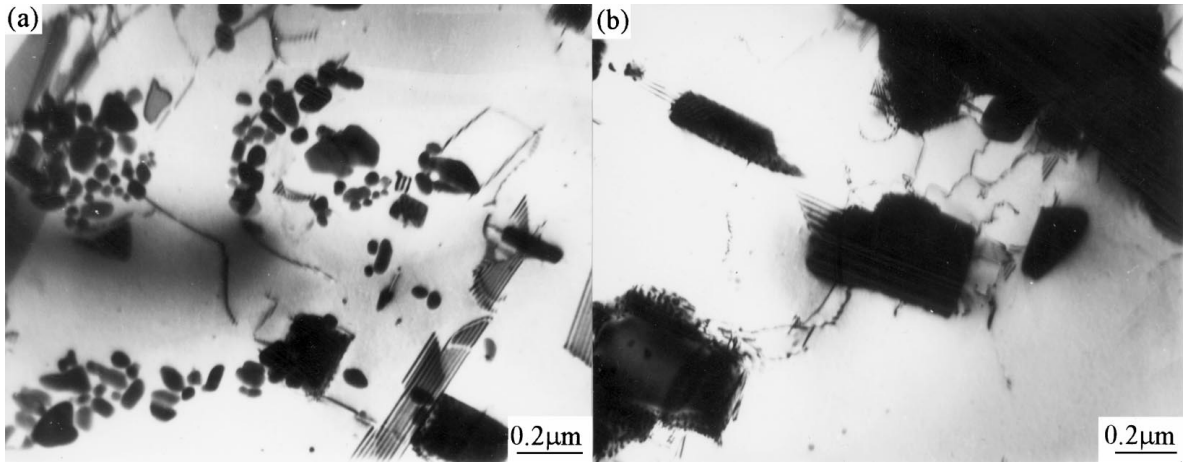

Figure 5 TEM micrographs showing the precipitation of $M_{23}C_6$ after test at $\sigma = 200$ MPa, $N_f = 1.92 \times 10^4$ cycles, on (a) dislocations and (b) stacking faults.

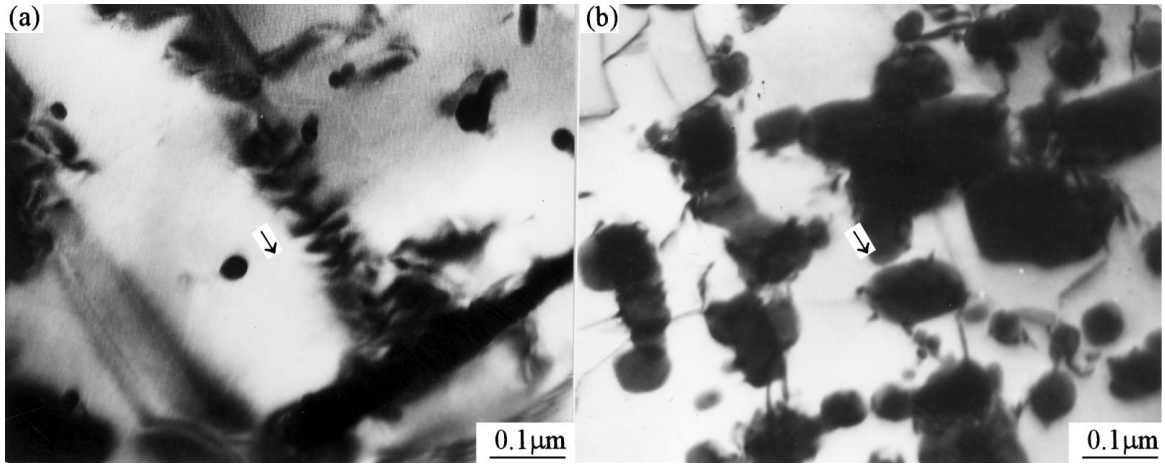

Figure 7 TEM displaying (a) deformation-induced dislocations in planar slip bands and pile-up of dislocations at secondary carbide in the interior of grains (b) uniformly distributed dislocations pinned up by fine secondary carbides in the vicinity of primary carbides after test at $\sigma = 200$ MPa, $N_f = 1.92 \times 10^4$ cycles.

3.2. Effect of carbides on deformation and fracture

During fatigue, the primary carbides decomposed sluggishly and secondary carbide precipitated profusively. The secondary carbide, $M_{23}C_6$, displayed a stronger interaction with dislocations. In the interior of grains, inhomogeneous deformation by means of planar slip is well developed and dislocations arranged themselves in planar array. The coarse secondary carbide precipitates distributed in grid form is a barrier of dislocation movement and caused the dislocation pile-up in the front of them, as shown in Fig. 7a. Undoubtedly, they played an important role in decreasing dislocation pile-up and reducing stress concentration. In the vicinity of primary carbides, deformation is homogeneous, for deformation-induced dislocations were pinned by the secondary carbide, as shown in Fig. 7b. Obviously, the dense distribution of fine precipitates is more effective in immobilization on dislocations. A homogenization of slip can enhance the elongation and ductility, since the local strain or stress can be relaxed by means of the homogeneous deformation, which may delay fracture. The profusive precipitation of $M_{23}C_6$ around the primary carbides avoided slip bands impinging on grain boundary, which would lead to boundary cracking [8].

A number of fine precipitates in the vicinity of the primary carbides are more effective in strengthening matrix than those coarse precipitates in the interior of grains. The deformation inhomogeneity of the alloy is attributed to uneven distribution of secondary carbide, which is an important immobilizing agent on dislocations, improving deformation resistance.

The secondary carbide not only restricts dislocation movement, but also hinder crack propagation. Fig. 8 shows that a secondary fatigue crack propagated and deflected by the secondary carbide. Due to the very small size of the secondary carbide, its effect on crack propagation is unobservable under SEM. This phenomenon could be defined as "crack deflection and meandering" [8]. As the fatigue crack advanced, $M_{23}C_6$ caused crack deflection and made the crack path much tortuous by $M_{23}C_6$ acting as an obstacle in the advance of the fatigue crack. It can be seen readily that the secondary

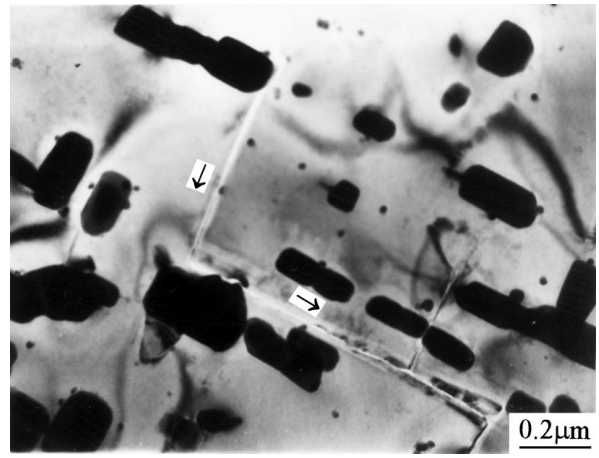

Figure 8 TEM showing deflection of crack propagation by the secondary carbides.

$M_{23}C_6$ carbide can improve not only deformation resistance but also fatigue crack propagation resistance.

Fracture observations by SEM show that fatigue cracks originated exclusively from specimen surface. The oxidized primary carbides on the surface of specimens acted as the site of fatigue crack initiation (Fig. 9a). As mentioned previously, during fatigue the primary carbides on the specimen surface were oxidized preferentially. The oxidization of carbides not only destroyed the surface continuity, but also prevented the secondary carbide precipitation in their vicinity which strengthened matrix, that results in crack initiation.

Fatigue crack propagation of the alloy is characterized by fatigue striations, as shown in Fig. 9b. Furthermore, it can be seen that primary carbides are an obstacle of crack propagation, deflecting cracks, which is confirmed by the formation of shear steps normal to the fatigue striations.

The present work indicates that carbides possessed an important role on deformation and fracture of the directionally solidified cobalt base superalloy during high temperature low cycle fatigue. The secondary carbides had a beneficial effect on improving deformation

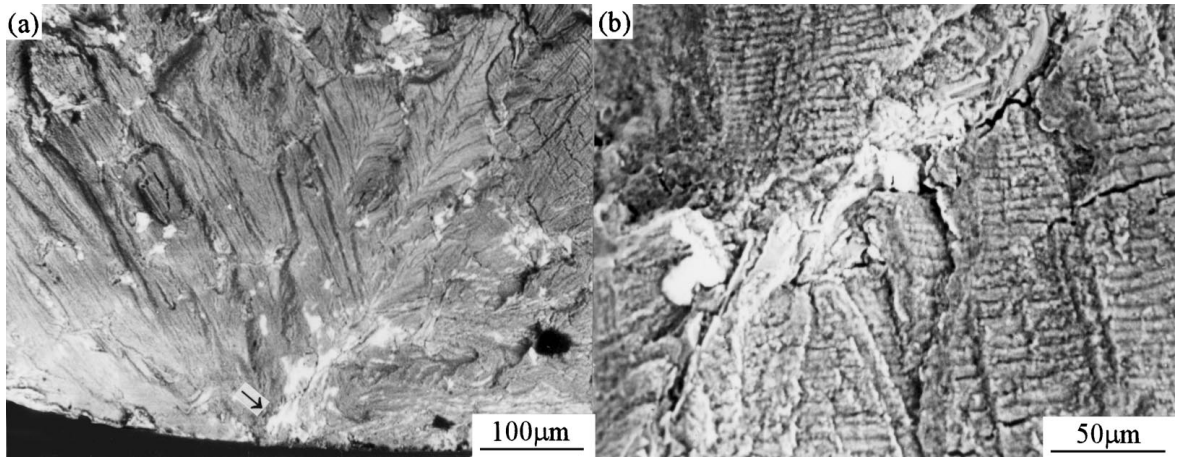

Figure 9 Scanning electron images showing (a) primary carbides on the surface of a specimen acted as crack initiation site and (b) fatigue striations and shear steps caused by prevention of the primary carbides to crack propagation.

resistance. Whereas, the primary carbides displayed dual roles. Those oxidized sites on the surface of specimen initiated crack. At the same time, those continuous networks around matrix were barrier for crack propagation and deflected cracks.

4. Conclusions

(1) During low cycle fatigue at 900 °C, the primary carbides M_7C_3 and MC decomposed sluggishly and a profusion of secondary carbide, chromium-rich $M_{23}C_6$, precipitated, which has a cube-cube orientation relationship with matrix.

(2) In the vicinity of the primary carbides, there is a dense distribution of fine $M_{23}C_6$, while in the interior of austenite grains they are scarce, coarse and aligned up, which are deformation-induced.

(3) Densely distributed fine $M_{23}C_6$ in the vicinity of the primary carbides pinned up dislocations effectively, resulting in a uniform distribution of dislocations. In the interior of grains, deformation was localized in slip bands, and coarse $M_{23}C_6$ precipitates are a barrier of planarly arranged dislocations. Also, they are an obstacle for crack propagation and deflect crack.

(4) Primary carbides on the surface of the specimen were oxidized preferentially, resulting in a precipitate-depleted zone around them. The oxidized carbides are crack initiation sites. The primary carbides at grain boundaries and interdendritic regions hindered crack propagation, causing the formation of shear steps.

References

1. C. T. SIMS, *J. Metals.* **21** (1969) 27.
2. S. D. ANTOLOVICH and N. JAYARAMAN, *Mater. Sci. Eng.* **57** (1982) L9.
3. W. H. JIANG, X. D. YAO, H. R. GUAN and Z. Q. HU, *Metall. Trans. A* **29A** (1999), in press.
4. C. T. SIMS and W. C. HAGEL, "The Superalloy" (John Wiley & Sons, New York, 1972) pp. 145–174.
5. R. F. VANDERMOUSEN, P. VIATOUR, J. M. DRAPIER and D. COUTSOURADIS, *Cobalt* **1** (1974) 6.
6. H. M. TAWANCY, *J. Mater. Sci.* **18** (1983) 2976.
7. J. R. LANE and N. J. GRANT, *Trans. ASM* **44** (1952) 113.
8. R. O. RITCHIE, *Mater. Sci. Eng.* **A103** (1988) 15.

Received 7 April 1998
and accepted 22 January 1999